Langevin Dynamics of the Choline Head Group in a Membrane Environment

Paul H. Konstant,* Linda L. Pearce,‡ and Stephen C. Harvey*‡
Departments of *Physiology and Biophysics and ‡Biochemistry and Molecular Genetics, University of Alabama at Birmingham, Birmingham, Alabama 35294 USA

ABSTRACT Computer simulations of dipalmitoylphoshatidylcholine (DPPC) have been performed using Langevin dynamics and a Marcelja-type mean field. This work has focused on the dynamics of the choline head group to parameterize the empirical constraints against phosphorus-carbon dipolar couplings ($D_{p\text{-}c}$) as measured by nuclear magnetic resonance (^{13}C-NMR). The results show good agreement with experimental values at constraints equivalent to the choline tilt observed in joint refinement of x-ray diffraction and neutron diffraction scatterings. Quadrupolar splittings for the α and β positions are also calculated and compared with ^{2}H-NMR experiments. The model predicts torsional transition rates around the α-β bonds and for the two C-O-P-O torsions. It also predicts T_1 relaxation times for the α and β carbons.

INTRODUCTION

Understanding of the structural characteristics of phospholipids that contribute to the properties of lipid bilayers has grown in recent years. Although experimental study of phospholipids in membranes has been difficult, some headway has been made. Previous work in nuclear magnetic resonance (^{2}H-NMR) focused on the dynamics of the acyl chains (Seelig and Seelig, 1980; Seelig and Waespe-Sarcevic, 1978; Smith and Oldfield, 1984). More recently, ^{13}C-NMR has allowed measurements of phosphorus-carbon dipolar couplings ($D_{p\text{-}c}$) in DMPC bilayers (Sanders, 1993). Additionally, joint refinement of x-ray and neutron scattering data has yielded detailed information on the coordinate distribution for both the head groups and acyl chains in DOPC bilayers (Wiener and White, 1992).

Recent ^{2}H-NMR has yielded an interesting functional response of choline head groups to bound surface charge (Seelig et al., 1987; Marassi and Macdonald, 1992). Binding cationic amphiphile to α-(β-) deuterated phosphatidylcholine bilayers results in a decrease (increase) in the quadrupole splitting. The exact opposite is seen upon binding anionic amphiphiles. Because phosphatidylcholine reports on surface charge via ^{2}H-NMR, it has been called a molecular voltmeter by Macdonald and coworkers (Macdonald et al., 1991). They have proposed a model for this phenomenon that quantifies the choline conformational change as a tilt in response to net surface charge. This has been named the choline tilt model. Most recently, Marassi and Macdonald (1992) have shown that the molecular voltmeter responds to microenvironments, not net surface charge, through the use of ternary mixtures of phosphatidylcholine, amphipathic anions, and amphipathic cations. In conclusion, they suggest modifying, but do not rederive, the choline tilt model to respond to local field environments.

These windows into phospholipid dynamics have been augmented in recent years by molecular dynamics (MD) simulations, which have demonstrated their utility in proteins and nucleic acids (McCammon and Harvey, 1987). In principle, MD simulations should be able to provide complete structural, dynamic, and thermodynamic information, if the potential energy functions can be made accurate enough. Several laboratories have carried out simulations on model membranes (Egberts and Berendsen, 1988; Damodaran et al., 1992; De Loof et al., 1991; Pearce and Harvey, 1993; Pastor and Venable, 1993; Venable et al., 1993; Heller et al., 1993). The long-term goal of such efforts would be to carry out MD simulations on a reasonably large patch of a fully solvated model membrane (containing several hundred lipid molecules and sufficient solvent molecules to cover the membrane to a depth of ~20 Å) over a time period long enough that all important motions would be represented (about 1 ms). Since current simulations cannot guarantee convergence in both time and space, one is forced to choose either a simulation on a large patch of membrane (but limited to a few hundred picoseconds) or a simulations covering a long time (but limited to a handful of molecules). Each approach has its advantages. The latter cannot be truly converged in space, but the former are not truly converged in time, since rotational diffusion of lipids occurs at rates slower than 1 ns^{-1}, as determined by NMR (Smith and Oldfield, 1984) and in MD simulations (De Loof et al., 1991; Pearce and Harvey, 1993; Venable et al., 1993), and translational diffusion is even slower (Smith and Oldfield, 1984). Figs. 2 and 5 of Venable et al. (1993) vividly shows the absence of these motions in subnanosecond MD simulations.

In terms of size, the most ambitious membrane simulations to date are those of Venable et al. (1993) and Heller et al. (1993). These include 72- and 200-phospholipid molecules, respectively, and a reasonable solvation layer. In terms of

Received for publication 21 July 1993 and in final form 28 April 1994.
Address reprint requests to Dr. Stephen C. Harvey, Department Biochemistry and Molecular Genetics, UAB Station 552 BHSB, University of Alabama at Birmingham, 1918 University Blvd., Birmingham, AL 35294. Tel.: 205 934 5028; Fax: 205 975 2547; E-mail: harvey@neptune.cmc.uab.edu.

0006-3495/94/08/713/07 $2.00

time, the most ambitious lipid simulations so far are those of DeLoof et al. (1989) and Pearce and Harvey (1993), which include only 1–7 molecules but cover tens of nanoseconds.

It is true that many measured parameters, such as NMR order parameters, do converge within the subnanosecond time scale accessible to simulations on large membrane patches. Parameters from those simulations also converge more rapidly than in our simulations, which is undoubtedly a manifestation of ergodicity, i.e., the statistics of averaging n molecules over t picoseconds is roughly equivalent to averaging one molecule over nt picoseconds. But there is a minimum time required for true convergence of any simulation, dictated by the slowest motions of the system. The fact that rotational and translational diffusion occur at rates slower than 1 ns^{-1} raise questions about the extent to which subnanosecond MD simulations on large systems are truly converged.

In the current study, we return to our single molecule DPPC model (De Loof et al., 1991) (Fig. 1 *A*) using Langevin dynamics and a Marcelja-type mean field to simulate the membrane environment. Our aim is to test the empirical constraints placed on the choline head group–tilt angle and harmonic motion around the average tilt angle–parameterizing against the recent measurements of $D_{p\text{-}c}$ (Sanders, 1993). In addition, we compare our results to the dynamic motion observed in joint refinement of x-ray and neutron diffraction data (Wiener and White, 1992). We also calculate the quadrupolar splittings for the α and β positions of the choline and compare them with the molecular voltmeter phenomenon and the choline tilt model. Finally, using the best parameter values, we use the model to calculate the spin-lattice relaxation times (T_1) for the head group carbons and to make predictions for torsional transition rates around the α-β torsion and the two C-O-P-O torsions (Fig. 1 *B*).

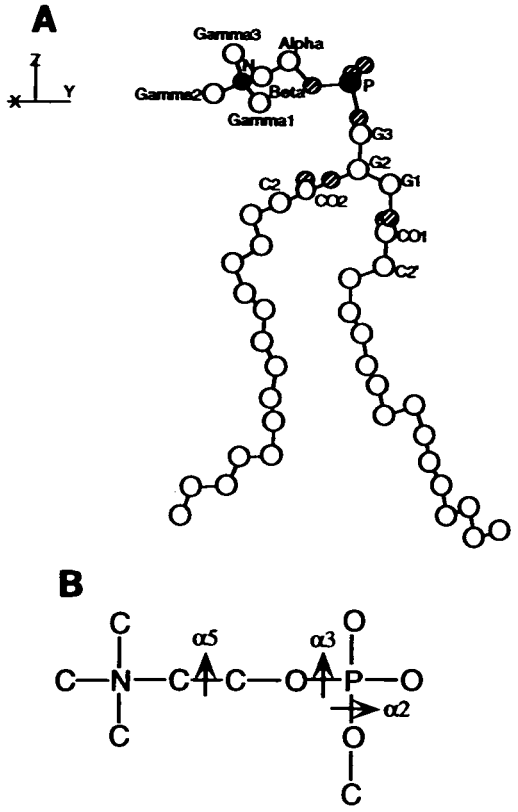

FIGURE 1 (*A*) Representative DPPC structure with head group, glycerol, and carbonyl carbons labeled. Nitrogen, phosphorus, and oxygen atoms are shaded. (*B*) Planar projection of head group with torsions of interest labeled in Sundaralingam's (1972) notation.

METHODS

Dynamics algorithm

The algorithm used for these simulations of single phospholipid molecules incorporates Langevin dynamics and a Marcelja-type mean field approximation as described previously (De Loof et al., 1991). The simulation temperature was 324 K, which is above the phase transition for DPPC (314.5 K). The Langevin dynamics algorithm (Brunger et al., 1984) requires a collision frequency which was set at 50 ps^{-1} as in previous simulations. The time step in these simulations was 2 fs.

Mean field model and other constraints

The Marcelja-type mean field (Marcelja, 1973; Pastor et al., 1988) has two terms, a repulsive term and a dispersive term, that remain unchanged from our previous work. The repulsive potential acts on the last carbon of the chain and is defined by

$$E_{rep} = \Sigma\Gamma/(z_{16}) \quad (1)$$

where Γ is the field strength set to -10.5 kcal/mol, z_{16} is the z position of the last carbon of the chain from the plane of the bilayer surface.

The dispersive term is a Maier-Saupe (1959) type potential, proportional to the molecular order parameter, $(3\cos^2\beta_i - 1)/2$, and simulates van der Waals interactions with neighboring lipid molecules. This term is defined by

$$E_{disp} = \Sigma - \Phi\tfrac{1}{2}(3\cos^2\beta_i - 1) \quad (2)$$

where Φ is the field strength, set to 0.21 kcal/mol; β_i is the angle between the bilayer normal and the vector normal to the plane defined by the two C-H vectors.

Additional constraints include a surface potential at -4 Å, which is used to keep the ends of the acyl chains from moving out of the bilayer, and empirical constraints on the head group which are under investigation in this paper. The phosphorus is held to the origin of coordinates by a tight harmonic constraint (k = 100 kcal/mol Å^2) that remained unchanged throughout. The nitrogen is held to defined z position (z_0), originally the xy plane, by an harmonic constraint given by

$$E(z) = \tfrac{1}{2}k(z - z_0)^2 \quad (3)$$

where k is the strength of the constraint in kcal/mol·Å^2. The distribution of the nitrogen position is then defined

by a Gaussian distribution with a mean of z_0 and a variance, $\sigma^2 = RT/k$, where R is the gas constant and T is the temperature. The goal of the present work is to find appropriate values of z_0 and k by varying them until the simulations produce calculated phosphorus-carbon dipolar coupling constants that agree with experimental values (Sanders, 1993). The strength of the constraint is reported as the standard deviation, σ, of the nitrogen motion as defined by the relationship above.

Starting structures and force potentials

Starting structures were derived from previous simulations of DPPC (De Loof et al., 1991) using a united atom model. The three γ CH_3 groups are reported as one average value. The potential function parameters were taken from the AMBER (Weiner et al., 1984) force field. Nonbonded interactions included only a 6–12 Lennard-Jones potential (cutoff 8 Å) and no electrostatics. Standard torsion potentials were used except for the alkane chains where a Ryckaert-Bellemans (1975) potential was used.

Simulation calculations

The $D_{p\text{-}c}$ values were calculated as (Sanders, 1993)

$$D_{p\text{-}c} = 12236 \cdot \langle (3\cos^2\theta - 1) \cdot r^3/2 \rangle \quad (4)$$

where r is the instantaneous internuclear distance, θ is the instantaneous angle between the internuclear vector and the bilayer normal, and the brackets denote a time-averaged function. As a first approximation of the error in the simulation, we calculated the root mean square deviation of the simulation values compared with experimental values. As a measure of the influence of each carbon position, we also calculated the root mean square deviation weighted by the relative error by the following:

$$\text{rms} = \Sigma(w_i(x_i^{\text{sim}} - x_i^{\text{exp}})^2/\Sigma w_i)^{1/2} \quad (5)$$

where w_i is a weighting factor equal to the reciprocal of the relative error squared ($w_i = 1/(\sigma_i^2/(x_i^{\text{exp}})^2)$) and σ_i is the experimental standard deviation for the ith carbon.

Quadrupolar splitting ($\Delta\nu$), as measured by ^{2}H-NMR, is calculated from the following (Seelig and Seelig, 1980)

$$\Delta\nu = 3/4(e^2qQ/h)S_{CD} \quad (6)$$

where e^2qQ/h is the static quadrupole coupling constant, which is 170 kHz for an aliphatic C-^{2}H bond, and S_{CD} is the order parameter (Seelig, 1977). This calculation was performed on the structures which were archived every 20 ps during the dynamics run, then averaged over the entire 100-ns simulation.

T_1 calculations

The relationship between experimentally determined NMR spin-lattice relaxation times (T_1) and the molecular motions can be determined from the following correlation function:

$$C(t) = 2/5\langle P_2[\mu(t) \cdot \mu(0)] \rangle \quad (7)$$

where P_2 is the second Legendre polynomial and μ is a unit vector pointing along a C-H bond (Lipari and Szabo, 1982). The ^{13}C spin-lattice relaxation can be calculated from:

$$\frac{1}{NT_1} = \left(\frac{h\gamma_C\gamma_H}{2\pi r^3}\right)^2 \frac{1}{10}[J(\omega_C - \omega_H) + 3J(\omega_C) + 6J(\omega_C + \omega_H)] \quad (8)$$

where N is the number of hydrogens bonded to the carbon, h is Plank's constant, r is the C-H bond distance (1.1 Å), γ_C, γ_H and ω_C, ω_H are the gyromagnetic ratios and Larmor frequencies of the ^{13}C and ^{1}H nuclei, and $J(\omega)$ is the spectral density of the $C(t)$ correlation function described above. Spectral densities were determined by curve fitting the first 5 ns of the correlation functions (see Table 3) (Pastor et al., 1988).

Computer resources

The molecular dynamics package was written in the C language as a modification of the yammp package (Tan and Harvey, 1993) by H. DeLoof. Calculations were performed on a hybrid Silicon Graphics 4D340GTX workstation or on a Silicon Graphics Indigo workstation. One nanosecond of simulation required about 2 h of CPU time on the 4D and 1 h on the Indigo.

RESULTS AND DISCUSSION

Because we are looking at the dynamics of a new region of the molecule, we re-examined the time to convergence for $D_{p\text{-}c}$ values. Fig. 2 *A* shows the time-averaged $D_{p\text{-}c}$ value for each successive nanosecond for the α carbon in the head group. This plot shows rapid convergence, which was typical for most of the carbons calculated. However, Fig. 2 *B* shows that $D_{p\text{-}c}$ values for G3, the glycerol carbon closest to the phosphorus, fluctuate substantially for about 50 ns. To assure adequate convergence, all simulations were run for 100 ns as in previous work.

Table 1 shows the results of $D_{p\text{-}c}$ calculations for the various series of simulations. As compared with experimental values in the top row, the first simulation result ($z_0 = 0 \pm 0.36$ Å) is analogous to the simulations reported previously (De Loof et al., 1991). Overall, $D_{p\text{-}c}$ values are in fair agreement for this simulation. The greatest error in the $D_{p\text{-}c}$ values for this simulation are in the α, β, and γ positions, whose values are about double the experimental values.

In the top series of experiments, we increased the σ of the nitrogen's motion keeping the mean nitrogen position constrained to the xy plane ($z_0 = 0$ Å). This series of simulations shows that under these conditions, the fit between simulation and experiment cannot be improved by varying the σ of the nitrogen's motion. At $\sigma = 1.47$ Å, we see some improvement in the unweighted rms deviation, but while the head group

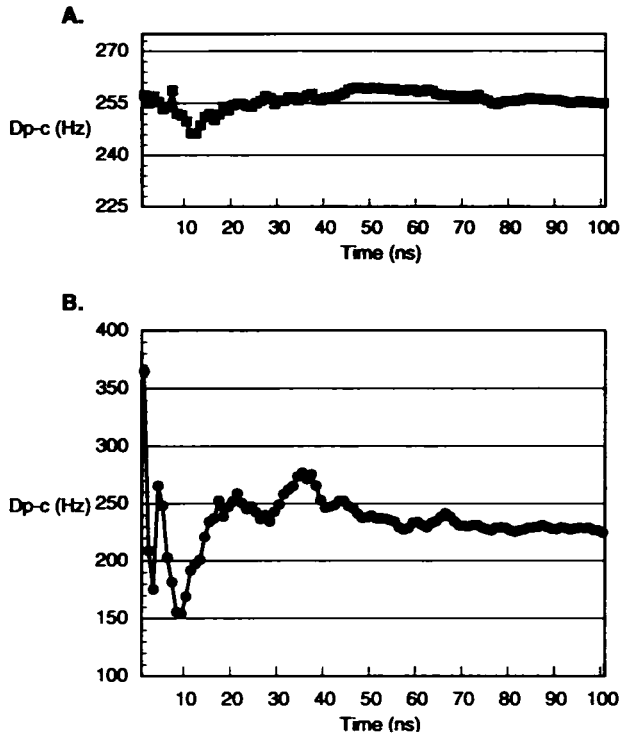

FIGURE 2 Cumulative average of $D_{p\text{-}c}$ values plotted against time for the α carbon (*A*) and the G3 glycerol carbon (*B*).

carbons have improved, the glycerol carbons have moved further from experimental values.

In the middle series of experiments, we retained the tight constraint (σ = 0.36 Å) and changed the average z position of the nitrogen. In this series, lowering the nitrogen below the xy plane has no clear effect on either the $D_{p\text{-}c}$ values or the rms deviations. Raising the nitrogen above the plane, on the other hand, clearly shows the head group $D_{p\text{-}c}$ values getting closer to experimental values from z_0 = 0.75 Å to z_0 = 1.5 Å, dropping below the experimental values from z_0 = 2.25 Å to z_0 = 3.0 Å. In joint refinement of x-ray diffraction and neutron diffraction scatterings, Wiener and White (1992) observed an average tilt of 22 ± 4°, which corresponds to 1.82 ± 0.33 Å. To compare our dynamics simulations, we ran two simulations at z_0 = 1.82 ± 0.36 Å and have reported their average, which shows excellent agreement in the $D_{p\text{-}c}$ values of the head group carbons and G3 as well as the lowest rms deviations of any of our simulations.

Using z_0 = 1.82 Å as the best value of nitrogen tilt, the bottom series of experiments shows the effect of loosening the constraint in the nitrogen. Again, little overall effect is seen. At z_0 = 1.82 ± 0.72 Å, little effect is seen at any carbon position; however, each small increase in deviation from the experimental values contributes to a rise in the rms deviation values. At this z_0 position, σ = 1.47 Å clearly reduces the agreement with experiment. This shows that, with z_0 = 1.82 Å, the optimum constraint force corresponds to σ = 0.36 Å, which demonstrates excellent agreement between simulation and experiment.

Overall, these results show a change in the tilt clearly improved the agreement with experimental $D_{p\text{-}c}$ values in all three head group carbons. It is interesting to note, however, that the behavior of the glycerol carbons is less clear. The $D_{p\text{-}c}$ values for G3 exhibits non-monotonic behavior with respect to both tilt and constraint strength, although most values are within experimental error. G2, on the other hand, is always below the experimental value and only once within experimental error at z_0 = −1.5 ± 0.36 Å. G1 similarly is always below experimental values, although a few of these values are within experimental error. This result can be interpreted in connection with the previous results for the order parameters for the first two carbons of the alkyl chains (De Loof et al., 1991). The S_{CD} values for these two carbons in both the sn-1 and the sn-2 chains showed the greatest deviation from experimental values. Here, we see consistent deviation in the glycerol carbons G1 and G2. Taken together, this implies that the current model shows significant deviation from experimental observation across the carbonyl carbons. This deviation could be the result of not representing the charge

TABLE 1 $D_{p\text{-}c}$ values for head group carbons from experiment (in parentheses) and simulation by series

z position (Å)	σ (Å)	CO1 (23 ± 4)	C2′ (ND)	G1 (62 ± 15)	G2 (141 ± 20)	CO2 (50 ± 8)	C2 (29 ± 8)	G3 (219 ± 30)	α (131 ± 20)	β (58 ± 15)	γ (<15)	rms*	Weighted rms‡
0.00	0.36	17.26	10.92	51.00	111.14	55.76	33.33	224.04	254.79	96.65	36.59	138	52.67
0.00	0.72	16.39	10.29	51.96	109.82	54.53	33.91	220.59	247.00	97.87	35.77	132	49.84
0.00	1.47	15.02	10.17	38.03	100.64	62.05	36.55	165.94	227.31	87.17	31.72	128	50.08
−1.50	0.36	15.27	10.52	38.43	122.03	75.54	42.36	154.39	223.05	76.70	24.67	123	49.63
−0.75	0.36	16.20	10.67	43.20	105.76	62.57	37.32	182.84	251.29	98.37	33.26	142	54.83
0.00	0.36	17.26	10.92	51.00	111.14	55.76	33.33	224.04	254.79	96.65	36.59	138	52.67
0.75	0.36	17.04	11.13	47.53	120.38	62.45	35.42	237.11	224.90	85.96	34.52	109	40.88
1.50	0.36	14.25	9.57	39.76	104.38	58.00	33.36	192.90	185.43	65.33	26.01	78	30.48
1.82	0.36	17.27	11.20	46.31	113.62	58.06	33.53	228.70	149.46	53.58	20.53	41	15.75
2.25	0.36	15.75	10.34	45.32	106.32	55.87	33.71	213.23	116.34	30.24	12.14	52	18.53
3.00	0.36	14.17	9.46	37.28	102.34	58.28	34.09	183.93	18.31	11.11	8.60	137	52.80
1.82	0.36	17.27	11.20	46.31	113.62	58.06	33.53	228.70	149.46	53.58	20.53	41	15.75
1.82	0.72	14.34	9.59	38.62	108.54	56.64	32.31	220.80	152.76	52.10	20.66	48	18.19
1.82	1.47	13.70	9.48	31.81	110.56	65.19	35.15	182.88	137.17	46.43	19.01	61	23.64

Top series: nitrogen z_0 = 0 Å with varied constraint force. Second series: varied mean nitrogen position, z_0, with σ = 0.36 Å. Third series: nitrogen z_0 = 1.82 Å with varied constraint force.

* Rms used γ = 15 Hz. Rms calculated from equation 5 with all weights w_i = 1.

‡ Weighted rms excluded γ position. Weighted rms calculated from Eq. 5 with weights inversely proportional to the relative experimental errors.

separation across the carbonyl group or the artificial constraint placed on the phosphorus.

Fig. 3 shows the calculated values for quadrupolar splittings over the range of mean nitrogen positions, z_0. Seelig et al. (1987) have shown that, in pure PC bilayers, $\Delta\nu_\alpha$ is 5.9 kHz and $\Delta\nu_\beta$ is 5.5 kHz. First, we see a much greater difference between the $\Delta\nu$ for the α and β positions than is observed experimentally. Secondly, the trends observed in Fig. 3 show that agreement between simulation and experimental values is not closest at $z_0 = 1.82 \pm 0.36$ Å, but somewhere between $z_0 = 1.82$ Å and $z_0 = 3.0$ Å.

In Fig. 3, we see that the $\Delta\nu$ values as a function of the mean nitrogen z position for both head group carbons parallel each other from a minimum at $z_0 = 3.0$ Å to a maximum at $z_0 = 0$ Å, then dropping again as z_0 drops to $z_0 = -1.5$ Å. Seelig and Macdonald (Seelig et al., 1987; Marassi and Macdonald, 1992; Macdonald et al., 1991) have observed that as the bound surface charge changes from negative to positive, $\Delta\nu_\alpha$ decreases and $\Delta\nu_\beta$ increases, the molecular voltmeter phenomenon. Macdonald et al. (1991) have interpreted their observations as choline tilt in response to surface charge. Our model shows that the molecular mechanics of choline tilting alone does not show the inverse relationship of $\Delta\nu_\alpha$ and $\Delta\nu_\beta$ of the molecular voltmeter. The possibility arises that the interaction of head groups with charge may produce more complex conformations than we observe with tilt alone. It must be noted that our model uses entirely empirical constraints on the choline—no charges or solvent are represented. Attempting to reproduce a phenomenon based on the interaction of charges with empirical constraints points out a limitation in the molecular mechanics model.

Table 2 shows predictions for torsion transitions, fraction of trans, gauche minus (g−), and gauche plus (g+) made from the simulation with the best agreement for $D_{p\text{-}c}$, $z_0 = 1.82 \pm 0.36$ Å. The table shows data for three torsional angles: O-C_α-C_β-N, C_{G3}-O-P-O and O-P-O-C_α, or, in Sundaralingam's notation (1972) α_5, α_2, and α_3, respectively.

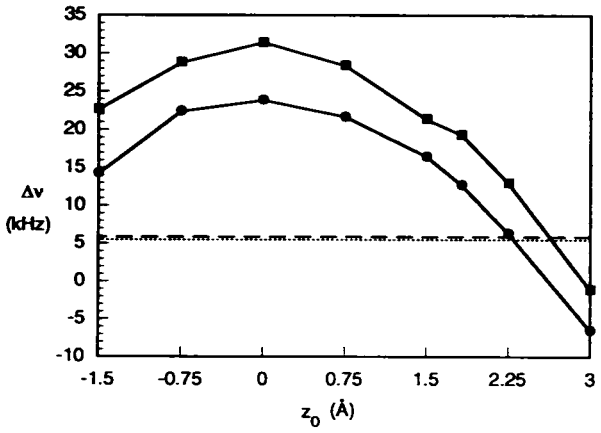

FIGURE 3 Quadrupolar splittings plotted against mean nitrogen position, z_0. Values calculated from archived structures, every 20 ps, shown with filled symbols (α = *squares*; β = *circles*). Experimental values shown as broken lines (α = *dashed*; β = *dotted*).

TABLE 2 Torsion transitions in selected head group torsions estimated by using the "simple counting" procedure (Loncharich et al., 1992)

	C-O-P-O α2*	O-P-O-C α3*	O-C-C-N α5*
Number of transitions			
t → g+	14	68	210
t → g−	64	63	244
g+ → t	16	71	210
g+ → g−	69	15	51
g− → t	61	61	244
g− → g+	71	17	51
Fraction			
g−	0.1771	0.4273	0.3093
t	0.3995	0.1771	0.4462
g+	0.4234	0.3957	0.2445
Transition rate (ns^{-1})			
t → g	1.95	7.40	10.17
g → t	1.28	1.60	8.20
g+ → g−	1.63	0.38	2.09
g− → g+	4.01	0.40	1.65

Number of transitions are given with fraction of trans, gauche minus (g−) and gauche plus (g+) and transition rates. Transition rates are calculated by (total number of transitions)/(total fraction of pertinent conformation)(simulation time).

* Sundaralingam's notation (1972).

For O-C_α-C_β-N, we see a significant rise in fraction of gauche to 0.55 from 0.25 seen for the acyl chains (De Loof et al., 1991). Additionally, there are significant transition rates for g+ → g− and g− → g+ due to the lack of hindrance from the oxygen.

For the C_{G3}-O-P-O torsion, we see lower transition rates and again a gauche conformation a majority of the time (0.60). For O-P-O-C_α, over 0.80 are in the gauche conformation and we see much lower g+/− → g−/+ transition rates. This is consistent with the crystal structure (Pearson and Pascher, 1979), which shows both of these torsions in the gauche conformation, and the energetics calculated from *ab initio* studies (Liang et al., 1993), which shows the gauche-gauche conformation to be a global minimum.

Experimental ^{13}C spin-lattice relaxation times (T_1 values) for C_α and C_β of the choline head group are 270 (±60) ms and 320 (±80) ms, respectively (Seelig and Seelig, 1980). Obtaining these T_1 values from our simulations, for comparison, involved the calculation of the reorientational relaxation of the carbon-hydrogen bond vectors in the laboratory frame and fitting the correlation function decays. As shown in Table 3, three exponentials were needed to adequately model the data. Goodness of fits were determined

TABLE 3 Details of three exponential fits of the P_2 correlation function for the two carbon-hydrogen vectors of the α and β carbons in the head group

		τ_1	τ_2	τ_3	a_1	a_2	a_3	τ
C_α	H1	4.74	34.6	445	0.590	0.160	0.249	119
	H2	5.39	71.6	822	0.269	0.549	0.181	190
C_β	H1	4.20	44.0	646	0.586	0.166	0.248	170
	H2	3.54	46.4	601	0.585	0.165	0.250	160

Time is in picoseconds. τ is a weighted average based on the three exponentials fits, $\tau = (a_1\tau_1 + a_2\tau_2 + a_3\tau_3)/(a_1 + a_2 + a_3)$.

by using a χ^2 test. Near-nanosecond time scale motions were observed and the predicted frequency dependence in the T_1 values calculated from our simulations is shown in Fig. 4. In comparison with the experimentally obtained data, we calculated T_1 values of 500 ms for C_α and 470 ms for C_β at the appropriate frequency. While the experimental and calculated T_1 values are within the same range, the relaxation times are somewhat longer in our model. This implies that the constraints placed on the phosphorus and nitrogen atoms restrict the motions about C_α (especially) and C_β and results in the slightly longer relaxation phenomena detected.

CONCLUSIONS

The empirical constraints placed on the head group of our DPPC model clearly yield parameters with good agreement to $D_{p\text{-}c}$ values measured experimentally (Sanders, 1993). Additional support for our constraint parameters, $z_0 = 1.82 \pm 0.36$ Å, is given by the agreement with data from the joint refinement of x-ray and neutron diffraction scatterings (Wiener and White, 1992) where the P-N tilt was calculated to be equal to $22 \pm 4°$, equivalent to 1.82 ± 0.33 Å. Analysis of the S_{CD} values for simulations with changes in the head group constraints show no significant changes from previously reported S_{CD}s in this system (De Loof et al., 1991) (data not shown). Although the current constraints do not represent the true interactions of the system, agreement with experimental measurements implies that we have succeeded in matching the average conformation and range of motion of the choline head group if not the exact dynamics of the molecule.

Calculated values of $\Delta\nu$ for the α and β carbons over a range of average z positions shows that under these empirical constraints $\Delta\nu_\alpha$ and $\Delta\nu_\beta$ parallel each other over the range of z_0 (Fig. 3). As a consequence, qualitative comparison of this result with the behavior observed by Seelig et al. (1987) shows that tilt alone cannot explain the inverse relationship between $\Delta\nu_\alpha$ and $\Delta\nu_\beta$ with bound surface charge known as the molecular voltmeter. This result calls into question the interpretation of the molecular voltmeter phenomenon known as the choline tilt model (Macdonald et al., 1991), implying that the change in head group dynamics seen with bound surface charge may produce a more complex conformational change than previously thought.

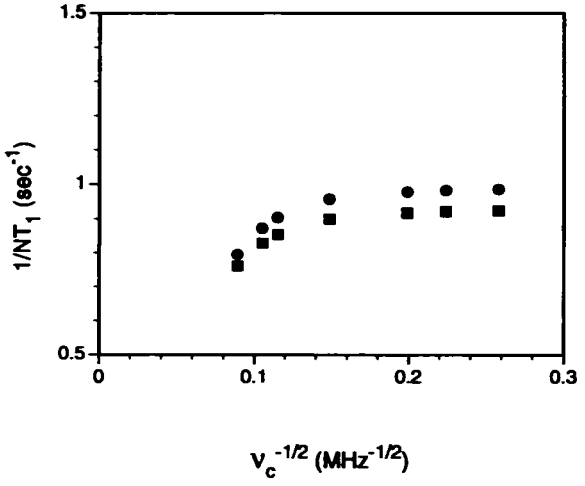

FIGURE 4 The frequency dependence of calculated T_1 values for the α and β carbons, with $1/NT_1$ plotted against $\nu_c^{-1/2}$ for ν = 15, 20, 25.15, 45.3, 75.5, 90.5, and 126 MHz. α = *squares*; β = *circles*.

We thank Dr. Jere Segrest for the generous donation of computer time on the Indigo and Dr. Richard Pastor for helpful discussions. We also thank Dvora Konstant for editing earlier versions of this manuscript.
This work was supported by Grant 2P01HL34343 from the National Institutes of Health.

REFERENCES

Brunger, A., C. B. Brooks, and M. Karplus. 1984. Stochastic boundary conditions for molecular dynamics simulations of ST2 water. *Chem. Phys. Lett.* 105:495–498.

Damodaran, K. V., K. M. Merz, and B. P. Gaber. 1992. Structure and dynamics of the dilauroylphosphatidylethanolamine lipid bilayer. *Biochemistry*. 31:7656–7664.

De Loof, H., S. C. Harvey, J. P. Segrest, and R. W. Pastor. 1991. Mean field stochastic boundary molecular dynamics simulation of a phospholipid in a membrane. *Biochemistry*. 30:2099–2113.

Egberts, E., and H. J. C. Berendsen. 1988. Molecular dynamics simulation of a smectic liquid crystal with atomic detail. *J. Chem. Phys.* 89: 3718–3726.

Heller, H., M. Schaefer, and K. Schulten. 1993. Molecular dynamics simulation of a bilayer of 200 lipids in the gel and in the liquid-crystal phases. *J. Phys. Chem.* 97:8343–8360.

Liang, C., C. S. Ewig, T. R. Stouch, and A. T. Hagler. 1993. Ab initio studies of lipid model species. 1. Dimethyl phosphate and methyl propyl phosphate anions. *J. Am. Chem. Soc.* 115:1537–1545.

Lipari, G., and A. Szabo. 1982. Model free approach to the interpretation of nuclear magnetic resonance relaxation in macromolecules: 1. Theory and range of validity. *J. Am. Chem. Soc.* 104:4546–4559.

Loncharich, R. J., B. R. Brooks, and R. W. Pastor. 1992. Langevin dynamics of peptides: the frictional dependence of isomerization rates of N-acetylalanyl-N′-methylamide. *Biopolymers*. 32:523–535.

Macdonald, P. M., J. Leisen, and F. M. Marassi. 1991. Response of phosphatidylcholine in the gel and liquid-crystalline states to membrane surface charges. *Biochemistry*. 30:3558–3566.

Maier, W., and A. Saupe. 1959. Eine einfache molecular-statictsche kristallinflussigen phase: teil I. *Z. Naturforsch. A.* 14:882–889.

Marassi, F. M., and P. M. Macdonald. 1992. Response of the phosphatidylcholine headgroup to membrane surface charge in ternary mixtures of neutral, cationic, and anionic lipids: a deuterium NMR study. *Biochemistry*. 31:10031–10036.

Marcelja, S. 1973. Molecular model for phase transition in biological membranes. *Nature*. 241:451–452.

McCammon, J. A., and S. C. Harvey. 1987. Dynamics of Proteins and Nucleic Acids. Cambridge University Press, Cambridge.

Pastor, R. W., and R. M. Venable. 1993. Molecular and stochastic dynamics simulation of lipid membranes. *In* Computer Simulation of Biomolecular Systems: Theoretical and Experimental Applications. W. F. van Gunsteren, P. K. Weiner, and A. K. Wilkinson. editors. ESCOM Science Publishers, Leiden. 443–463.

Pastor, R. W., R. M. Venable, M. Karplus, and A. Szabo. 1988. A simulation based model of NMR T1 relaxation in lipid bilayer vesicles. *J. Chem. Phys.* 89:1128–1140.

Pearce, L. L., and S. C. Harvey. 1993. Langevin dynamics studies of unsaturated phospholipids in a membrane environment. *Biophys. J.* 65:1084–1092.

Pearson, R. H., and I. Pascher. 1979. The molecular structure of lecithin hydrates. *Nature*. 281:499–501.

Ryckaert, J. P., and A. Bellmans. 1975. Molecular dynamics of liquid *n*-butane near its boiling point. *Chem. Phys. Lett.* 30:123–125.

Sanders, C. R. 1993. Solid state ^{13}C NMR of unlabeled phosphatidylcholine bilayers: spectral assignments and measurement of carbon-phosphorus dipolar couplings and ^{13}C chemical shift anisotropies. *Biophys. J.* 64: 171–181.

Seelig, J. 1977. Deuterium magnetic resonance: theory and application to lipid membranes. *Q. Rev. Biophys.* 10:353–418.

Seelig, J., P. M. Macdonald, and P. G. Scherer. 1987. Phospholipid head groups as sensors of electric charge in membranes. *Biochemistry* 26: 7535–7541.

Seelig, J., and A. Seelig. 1980. Lipid conformations in model membranes and biological membranes. *Q. Rev. Biophys.* 13:19–61.

Seelig, J., and N. Waespe-Sarcevic. 1978. Molecular order in cis and trans unsaturated phospholipid bilayers. *Biochemistry.* 17:3310–3315.

Smith, R. L., and E. Oldfield. 1984. Dynamic structure of membranes by deuterium NMR. *Science.* 225:280–288.

Sundaralingam, M. 1972. Molecular structures and conformations of phospholipids and sphingomyelins. *Ann. N.Y. Acad. Sci.* 195: 324–355.

Tan, R. K.-Z., and S. C. Harvey. 1993. Yammp: development of a molecular mechanics program using the modular programming method. *J. Comp. Chem.* 14:455–470.

Venable, R. M., Y. Zhang, B. J. Hardy, and R. W. Pastor. 1993. Molecular dynamics simulations of a lipid bilayer and of hexadecane: an investigation of membrane fluidity. *Science.* 262:223–226.

Weiner, S. J., P. A. Kollman, D. A. Case, U. C. Singh, C. Ghio, G. Alagona, S. Profeta, and P. Weiner. 1984. A new force field for molecular mechanical simulation of nucleic acids and proteins. *J. Am. Chem. Soc.* 106:765–784.

Wiener, M. C., and S. H. White. 1992. Structure of a fluid dioleoylphosphatidylcholine bilayer determined by joint refinement of x-ray and neutron diffraction data III. Complete structure. *Biophys. J.* 61:434–447.